Electronic Supplementary Information (ESI)

Deep, sub-wavelength acoustic patterning of complex and non-periodic shapes on soft membranes supported by air cavities

Kuan-Wen Tung[a], Pei-Shan Chung[b], Cong Wu[g], Tianxing Man[a], Sidhant Tiwari[c], Ben Wu[bdef], Yuan-Fang Chou[h], Fu-ling Yang[h], Pei-Yu Chiou*[ab]

[a] *Department of Mechanical and Aerospace Engineering, University of California at Los Angeles, 420 Westwood Plaza, Los Angeles, CA 90095, USA.*
[b] *Department of Bioengineering, University of California at Los Angeles, 410 Westwood Plaza, Los Angeles, CA 90095, USA.*
[c] *Department of Electrical and Computer Engineering, University of California at Los Angeles, 420 Westwood Plaza, Los Angeles, CA 90095, USA.*
[d] *Department of Materials Science and Engineering, University of California at Los Angeles, 410 Westwood Plaza, Los Angeles, CA 90095, USA.*
[e] *Division of Advanced Prosthodontics, School of Dentistry, University of California at Los Angeles, 714 Tiverton Ave, Los Angeles, CA 90024, USA.*
[f] *Department of Orthopedic Surgery, School of Medicine, University of California at Los Angeles, 10833 Le Conte Ave, Los Angeles, CA 90095, USA.*
[g] *Department of Mechanical and Biomedical Engineering, City University of Hong Kong, Tat Chee Ave, Kowloon Tong, Hong Kong.*
[h] *Department of Mechanical and Aerospace Engineering, National Taiwan University, No. 1, Section 4, Roosevelt Rd, Da'an District, Taipei City, Taiwan 10617.*

*Email: pychiou@g.ucla.edu

This ESI file includes:

Figs. S1 to S3
Captions for movies S1 to S6

Other supplementary materials for this manuscript include the following:

Movies S1 to S6

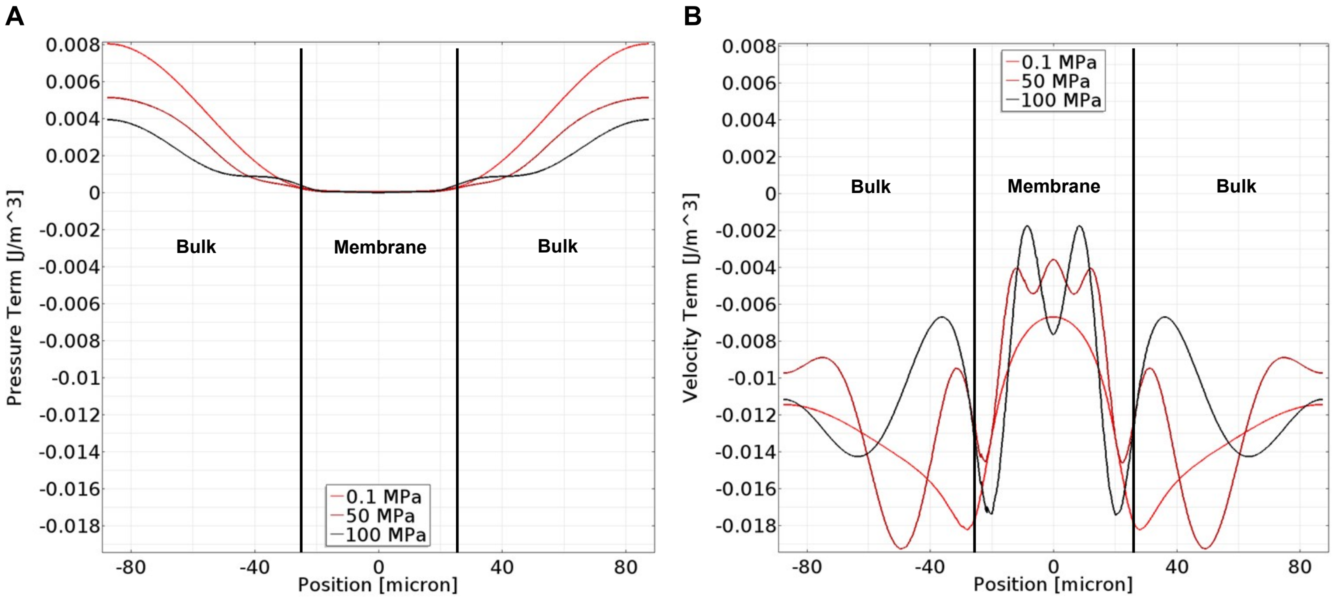

Fig. S1. Analysis of the contributing factors to the resulted acoustic potential profile of Fig. 2C. The pressure term $\frac{1}{2}\kappa_o < p^2 >$ (*A*) of the radiation potential equation (1b) shows same trend across the entire range of E' examined such that the pressure decreases from the maximum outside the membrane region to the minimum at the center. On the other hand, the velocity term $-\frac{3}{4}\rho_o < v^2 >$ (*B*) of equation (1b) shows variations across the range of E', except at the edges of membrane region where largest amplitude occur. The higher the E' is the stronger the fluctuation of the velocity term becomes. In all cases, largest velocity amplitude occurs at the membrane edges. Of note is that the relative contributions of these terms on the radiation potential profile needs to consider the f_1 and f_2 factors that represent particle's properties but not included here.

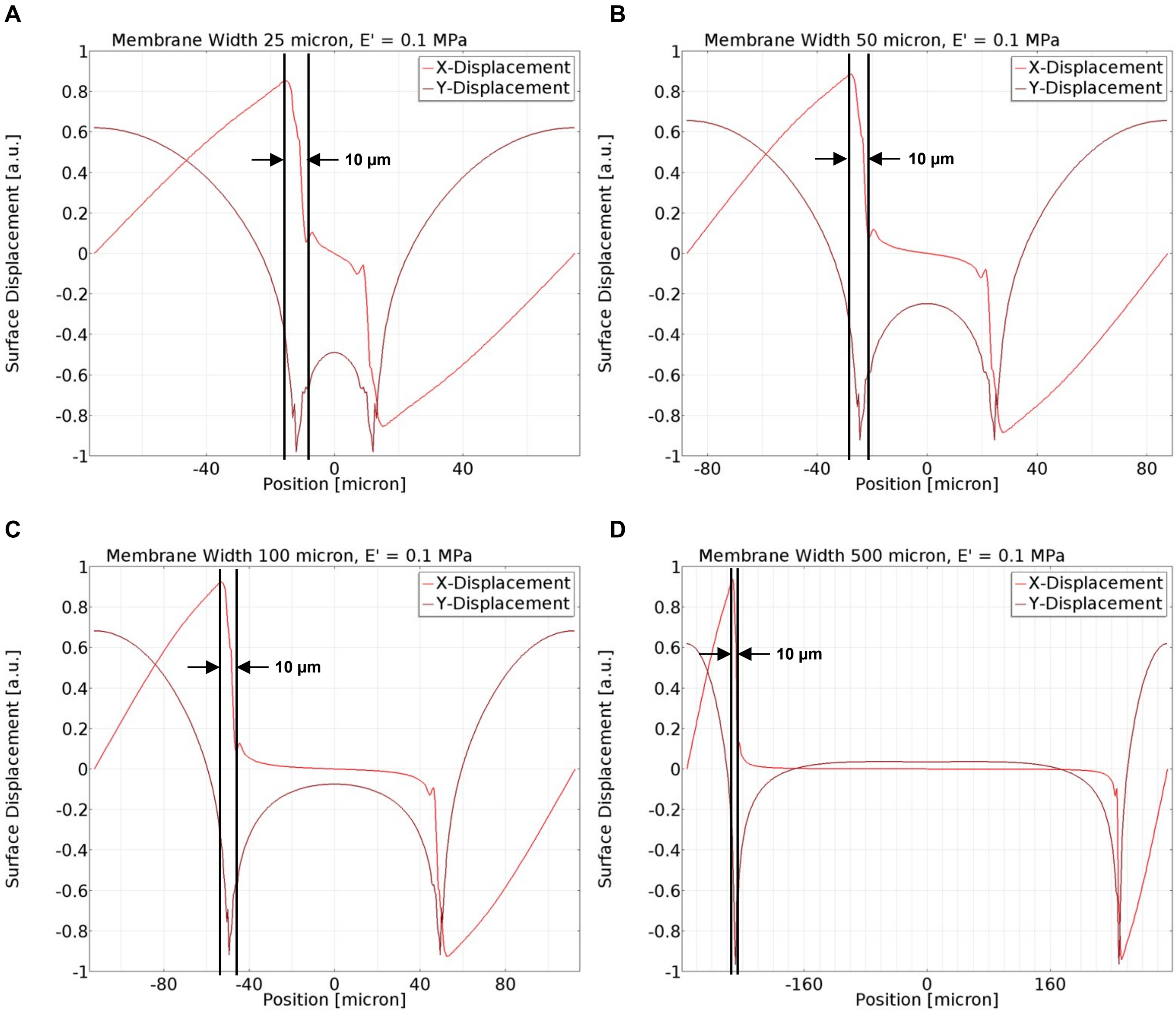

Fig. S2. Simulated surface displacements of soft, air-embedded PDMS structure with varying air cavity widths. To determine the length of wave decay from the bulk into the membrane region, we explore different widths of air cavity sized from 25 μm to 500 μm (*A*-*D*), assuming the structure of E' of 0.1 MPa, following the simulation model in Fig. 2. Results show that, regardless of the membrane sizes, wave propagating from the bulk decays in ~10 μm.

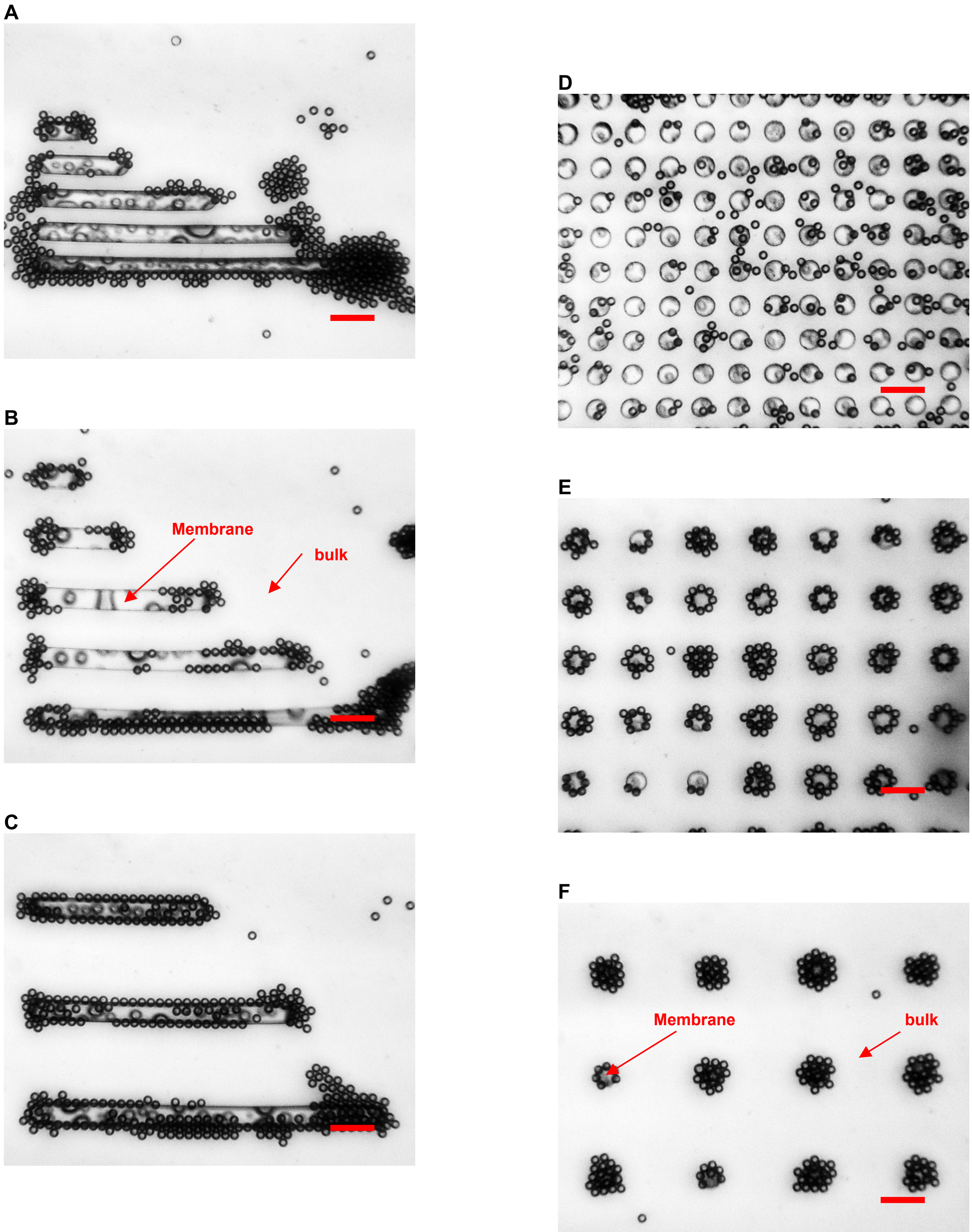

Fig. S3. Patterning of microparticles in water using soft, air-embedded PDMS structures in the shape of strip and circle. Under the excitation of 3 MHz and 5 V_{rms}, stripped-structures spaced at 25 µm (*A*), 50 µm (*B*), and 100 µm (*C*) are used to pattern 10 µm polystyrene beads. Results show that trapping pattern gets distorted at the spacing of 20 µm, indicating the CMAP's spatial resolution at 50 µm. Equivalently, patterning using circular-structures spaced at 25 µm (*D*), 50 µm (*E*), and 100 µm (*F*) show the best spatial resolution at 50 µm. Scale bar, 50 µm.

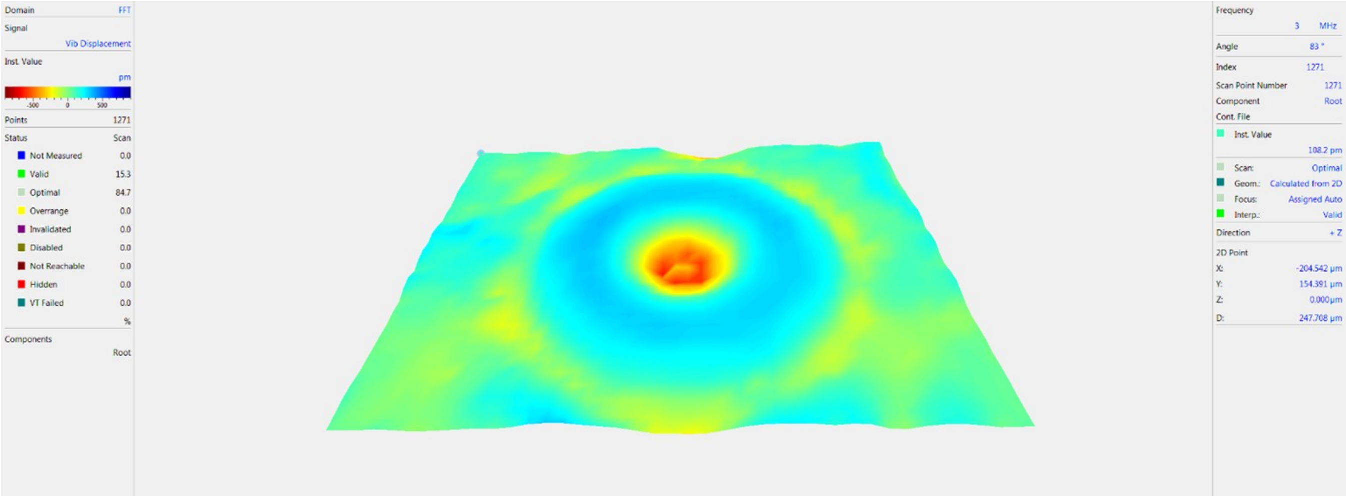

Movie S1. LDV measurement over a cycle of acoustic excitation at 3MHz on the surface of the hard, air-embedded PDMS concentric ring-structure that interfaces the above fluid is performed. High-order structure vibration mode is observed at the very center of the circular membrane.

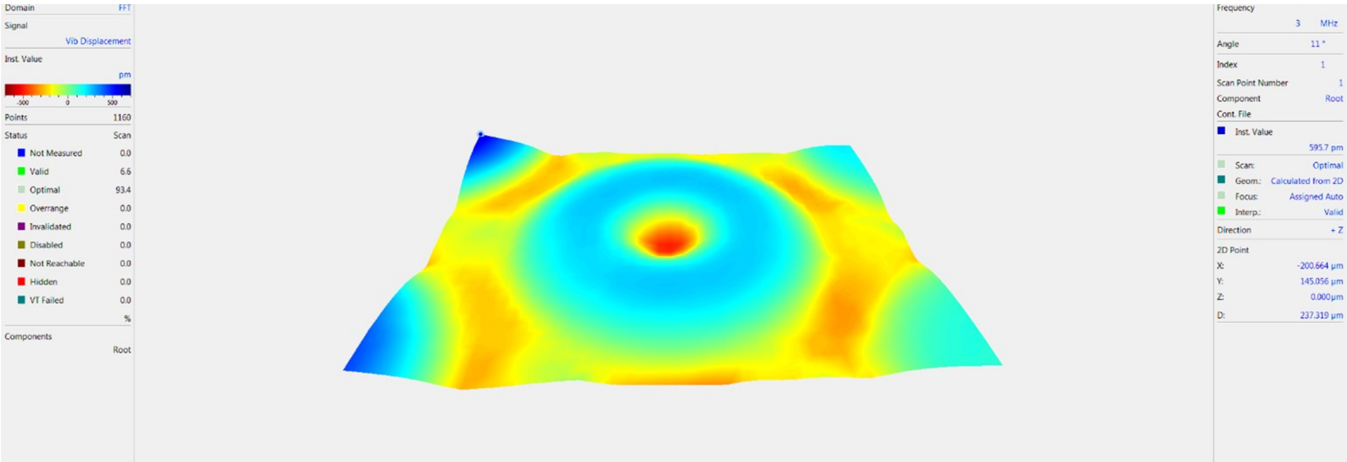

Movie S2. LDV measurement over a cycle of acoustic excitation at 3MHz on the surface of the soft, air-embedded PDMS concentric ring-structure that interfaces the above fluid is performed. At the very center of the circular membrane, the profile is smooth and shows no high-order structure vibration mode.

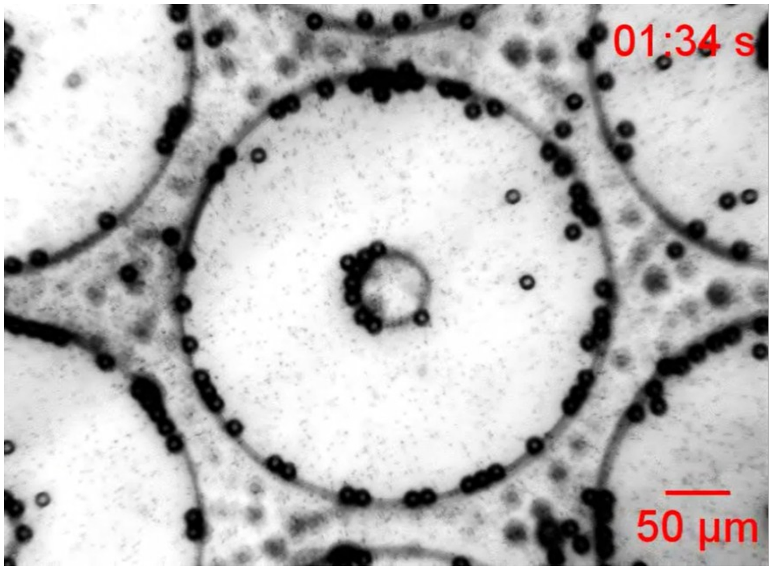

Movie S3. 10 µm and 1 µm polystyrene beads in water are patterned using the soft, air-embedded PDMS concentric ring-structure at the acoustic excitation of 3 MHz and 5 V_{rms}. The 10 µm beads migrate toward and reside at the edges of PDMS membrane. However, the 1 µm beads near the edge of the center, circular membrane form vortex patterns of approximately 25 µm in width. Such patterns are quickly overcome by the bulk movement, referred as global flow, across the entire device.

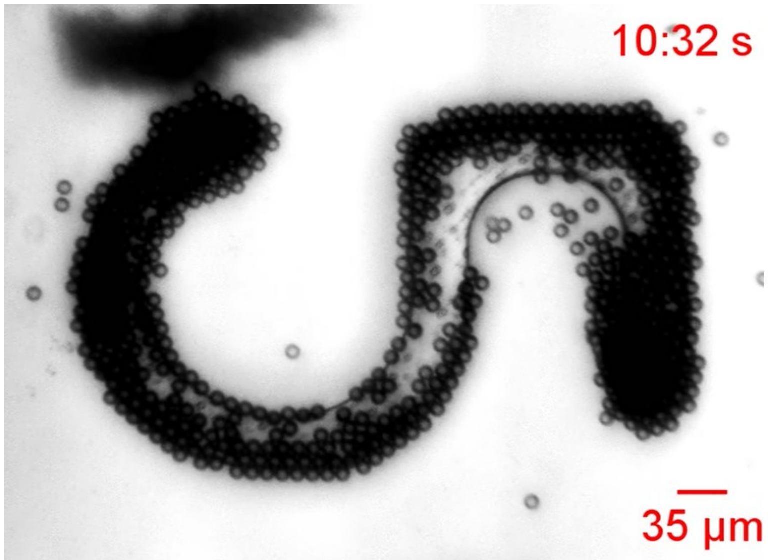

Movie S4. 10 μm polystyrene beads in water are patterned using the soft, air-embedded PDMS structure consisted of numeric character “5” at the acoustic excitation of 3 MHz and 5 V_{rms}. High concentration of the beads leads to filling of the region above the PDMS membrane, conforming to the shape of air cavity. Notice that the beads flowing outside the cavity are the excessive targets to what the potential well above the cavity can hold.

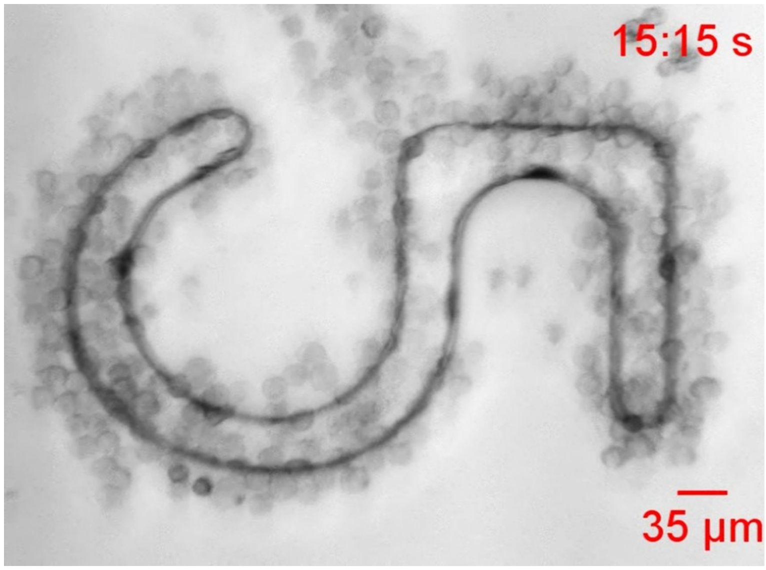

Movie S5. HeLa cells in DMEM are patterned using the soft, air-embedded PDMS structure consisted of numeric character “5” at the acoustic excitation of 3 MHz and 5 V_{rms}. High concentration of the cells leads to filling of the region above the PDMS membrane, conforming to the shape of air cavity. Notice that the cells flowing outside the cavity are the excessive targets to what the potential well above the cavity can hold.

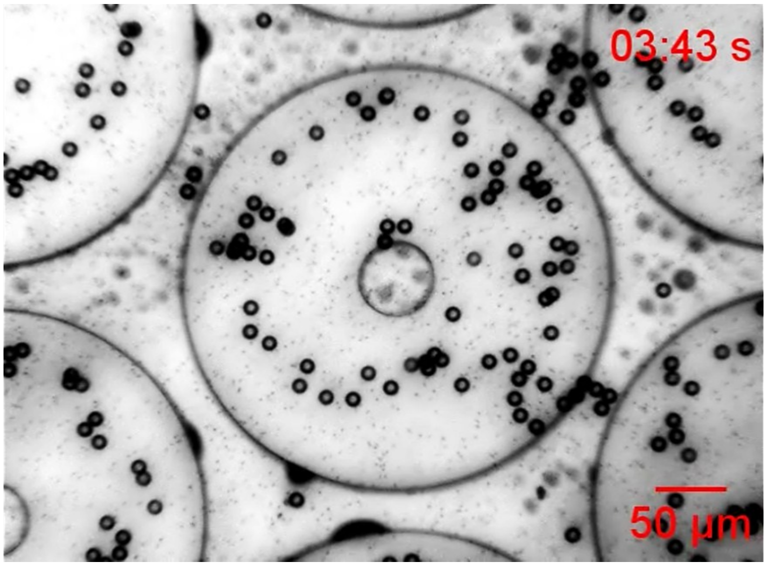

Movie S6. Patterning of microparticles in water using soft, air-embedded PDMS structures in the shape of concentric rings. Under the acoustic excitation of 0.5 MHz 12.5 V_{rms}, acoustic streaming flow is induced as shown by both the 1 and 10µm polystyrene beads circulating in vortices. This flow is very noticeable at the most center structure.